Departament d'Enginyeria Química
Escola Tècnica Superior d'Enginyeries
Universitat Autònoma de Barcelona
Tel.: 93.581.10.18 Fax: 93.581.20.13
08193 Bellaterra Spain

MELISSA

Memorandum of Understanding

ECT/FG/MMM/97.012

Contract Number: ESTEC/CONTRACT13292/98/NL/MV

Technical Note: 66.2

Bench scale loop tests using artificial medium

Version: 1

Issue: 0

CREUS N.; ALBIOL, J.; GODIA, F.

December 2002

Document Change Log

Version	Issue	Date	Observations
Draft	0	15/07/02	Preliminary Version
1.0	0	15/12/02	Final Version

Table of Contents

1 INTRODUCTION

The MELISSA project (Microbiological Ecological Life Support System Alternative) of the European Space Agency (ESA) is devoted to the development of a biological life support system to be used during long term Manned Space Missions. In order to achieve this purpose the project proposes the connection between five compartments, four of which contain microbial organisms and one higher plants and algae.

The liquefying compartment, or compartment I, is responsible for the biodegradation of human faecal material and other wastes generated by the crew. The volatile acids, ammonium, gases and soluble components produced during the fermentation are fed into the second compartment.

The anoxygenic phototrophic compartment II metabolises some of the compounds produced in the anaerobic liquefying compartment, with edible biomass generation. To achieve this goal *Rhodospirillum rubrum* and *Rhodobacter capsulata* are cultured in an anaerobic environment, either in photoheterotrophic or in photoautotrophic conditions.

The objective of compartment III (nitrifying compartment) is to transform the ammonium ions present in the exit stream from compartment II into nitrate, the most appropriate nitrogen source assimilated by the cells cultured in compartment IV. It consists in a packed-bed reactor with cells of two bacterial strains (*Nitrosomonas europaea* and *Nitrobacter winogradskyi*) immobilized onto polystyrene beads (Biostyr).

Compartment IVa has as its main task the carbon dioxide removal and supply of oxygen for the crew respiration generating at the same time edible biomass as food supply. This compartment is currently implemented in airlift reactors where *Spirulina platensis* is cultivated. This cyanobacteria presents a high nutritional value and contains all the essential amino acids, besides cysteine, in the adequate concentrations according to the FAO proposed standards.

The higher plants compartment is the basic food supplier for the crew. This compartment is being preliminary designed and some studies are being done with the candidate crops.

To assure the satisfactory operation of the system, it is important to study the connection between these bioreactors not only at optimal conditions but also taking into account possible deviations in the behaviour of any of them.

Dynamic operation of a loop of bioreactors will result in transitory states, especially when the system is driven from one steady state to another one or due to an eventual malfunction. In these cases, incomplete consumption of substrates may result and the effect of those on the subsequent bioreactors must be well characterized in order to foresee their behaviour and ensure the proper operation of the loop.

Once this study has been successfully done in the connection of compartments II, III and IVa using acetic acid or a mixture of acetic, propionic and butyric acids as carbon source (Creus et al., 1999; Creus et al., 2001; Creus et al., 2002a), a closer approach to the future operation of the whole connection of the loop had to be carried out.

Continuation of the operation of the liquid interconnection of compartments II, III and IVa is presented in this work. For this, the tests are performed using an artificial media simulating the media outcoming from compartment I. Once the proper operation of the connection in these conditions will have been tested, the whole loop liquid connection will be done using output medium of compartment I from Gent (Creus et al., 2002b). If the complete loop of microbial bioreactors can be operated satisfactorily in all those cases, then the feasibility of the connection of the MELISSA loop at liquid phase level will be demonstrated.

2 SET-UP AND MATERIALS AND METHODS

Since at the time of the realisation of this work compartment I was being developed by EPAS, (one of the MELISSA partners in Gent (Belgium), an approach to the outlet medium from compartment I using artificial medium was used. However one important difference among these tests and the previous ones was that the light available in the bioreactor used was higher than in any previous test. A brief description of the used medium, of each compartment and the different steps required in their connection are given in this section.

2.1 Compartments Set-Up

The general view of the experimental set up of compartments II, III and IVa, placed in Barcelona, and the necessary separation units to connect them are shown in figure 2.1.

2.1.1 Compartment II

Cultures corresponding to the second compartment are done in a 0.5 L tank bioreactor (BIOSTAT Q, Braun Biotech International). A pH control unit (CRISON pHrocon 18) regulates the pH of the culture media at 6.9 by addition of acid (HCl 1M) or base (NaOH 1.5M). A magnetic stirrer, set at 600 rpm, is used to ensure the perfect mixing of the culture.

A constant CO_2 flow, varying from 0.75-2.24 mL/min, depending on the cultures conditions, is bubbled to the culture providing anaerobic conditions and CO_2-carbon source, which is required in order to degrade all the volatile fatty acids present in the incoming media. The temperature, set at 30ºC, is controlled by an external water jacket.

Illumination of the bioreactor is obtained using 18 halogen lamps (*SYLVANIA* Halogen –Professional de luxe-, 12V, 20W, ∅ 50mm.) distributed, radially around the external wall, in 6 columns containing, each one, 3 lamps. One 15V–40A power supply provides the necessary electrical power. Changing the voltage supplied to the lamps, the light intensity is modified. A calibration of the light intensity in W/m^2 at the surface of the reactor as a function of the voltage is given in Appendix I. A picture of this compartment is provided in figure 2.2.

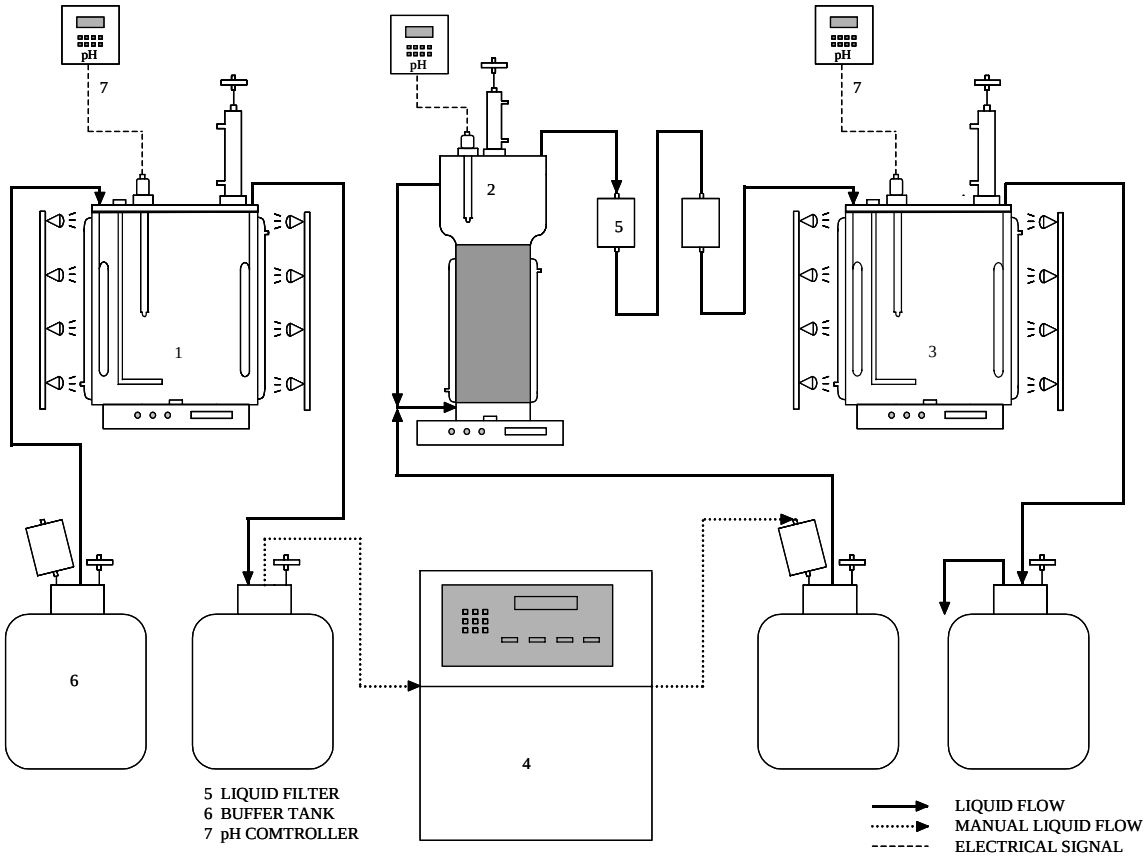

Figure 2.1. - Diagram of the experimental set up for the liquid connection of compartments II, III and IVa of MELISSA loop .

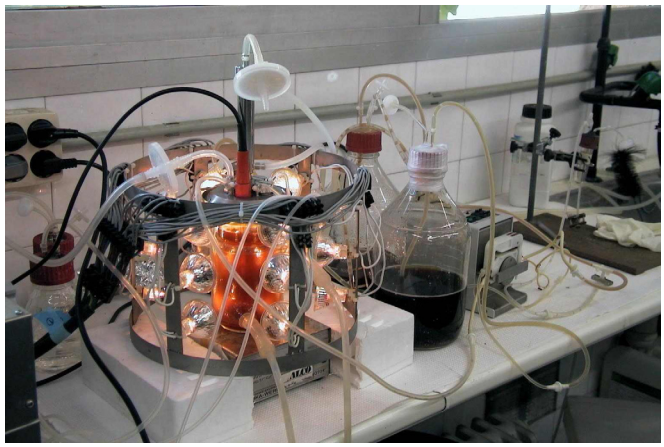

Figure 2.2.- Picture of compartment II. MELISSA effluent of compartment I is used as incoming media.

2.1.2 Connection between compartment II and III

Due to the fact that the outlet of compartment II contains biomass, a biomass removal step is necessary. To this purpose a centrifugation step is introduced in the liquid effluent of compartment II previous to the transfer operation to compartment III. The volumes managed during the continuous runs at bench scale, are too small to use a continuous centrifuge. Thus, a batch centrifuge (BECKMAN J2-21 M/E) (10000rpm,

4ºC, 20min) is used. As the centrifugation operation is a discontinuous process, two buffer tanks, one for the outlet of compartment II and the other for the inlet of compartment III are required. Then the collection of the liquid effluent for centrifugation and the storage of the biomass free medium after the centrifugation step are allowed. This centrifugation step is done daily as the quality of Rhodospirillum rubrum decreases significantly when it is stored during a longer period.

To avoid contamination of the centrifuged media, sterilization before introducing it to the input storage tank of the third compartment is required. To this purpose a filtering step, using liquid filters (MILLIPORE OPTICAP^{TM} 4") of 0.22µm, is introduced.

2.1.3 Compartment III

Implementation of compartment III is done using a packed-bed column, as described previously in TN 37.510 (Pérez et al., 1997).

The pH is controlled by an autonomous controller (CRISON pH/mV 252). Regulation of the pH at 8.4, is achieved by means of acid (CO_2) or base (Na_2CO_3 40g/L) addition. Temperature is controlled at 30ºC by an external water jacket. Aeration is done through a gas sparger. Part of the effluent of the bioreactor is recirculated in order to achieve a higher conversion. A magnetic stirrer is used to ensure the perfect mixing between the inlet and the recirculation. A picture of this compartment is found in figure 2.3.

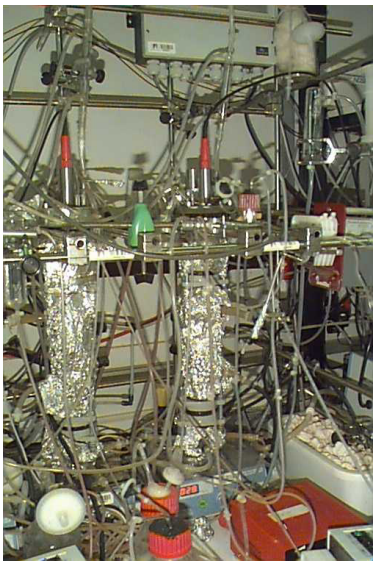

Figure 2.3.- Picture of compartment III.

2.1.4 Connection between compartments III and IVa

These two compartments can be directly connected. However, due to the fact that the outlet of compartment III can contain some biomass (basically: cells leaked out from the biofilm structure), two filtering steps through liquid filters (MILLIPORE OPTICAP^{TM} 4") of 0.22μm are included. One is located at the output of compartment III and another one at the input of compartment IV. In this way, the two compartments are isolated allowing a disconnection in case of a potential malfunction of one of them.

2.1.5 Compartment IVa

The same equipment used in compartment II is used in compartment IVa. A calibration of the light intensity in W/m^2 at the surface of the reactor as a function of the voltage is given in Appendix II. A picture of this compartment is found in figure 2.5.

Figure 2.4.- Picture of compartment IVa.

2.2 MATERIALS AND METHODS

2.2.1 Strains and inoculum

The strain of *Rhodospirillum rubrum* used (ATCC 25903) is obtained from the American Type Culture Collection. It is revived and the subcultures are done using their recommended medium. The inoculum volume is fixed as the 10% of the working volume.

The strains of *Nitrosomonas europaea* and *Nitrobacter winogradsky*i used are obtained from the American Type Culture Collection: *Nitrosomonas europaea* (ATCC 19718) and *Nitrobacter winogradsky*i (ATCC 25391). A co-culture (*Nitrosomonas*

europaea and *Nitrobacter winogradsky*i) obtained from the operation of a Biostat B reactor (Pérez *et al*., 1997) is used to inoculate the reactor.

The *Spirulina platensis* strain used is obtained from the Pasteur Institute*: Arthospira platensis* (PCC 8005). *S. platensis* is revived and the subcultures are done using their recommended medium. The inoculum's volume is fixed as the 10% of the working volume.

2.2.2 Analytic procedures

2.2.2.1 Cell concentration

- Dry weight

S. platensis and *R. rubrum* dry weight are determined by filtering through a 1.2μm and 0.22μm respectively pre-weighted filters, dried until constant weight in a microwave (20 min., 150 W) and cooled down in a desiccator.

- Optical density

The optical density measured at 750nm and 700nm is a direct measurement respectively of the *S. platensis* and *R.rubrum* concentration. Polysaccharides do not absorb at these wavelengths. Thus, these measurements reflect only the diffusion of the light produced by the presence of the microorganisms, fact that is directly related with biomass concentration. The spectrophotometer used is a Kontron Instrument, Uvikon 941, Italy.

2.2.2.2 Ammonium, nitrite and nitrate concentrations

- Ammonium

Ammonium was measured using UV measurement determinations by means of LCK 305 ammonium analysis kits (Dr. Lange Nitrax).

BASIS: Ammonium ions react with the hypochloride and salicylate ions in presence of nitroferrocyanide. Nitroferrocyanide acts as a catalyser (pH=12.6) forming iodophenol blue. Iodophenol blue is quantified measuring the absorption at 694nm.

- Nitrate

Nitrate is measured using UV measurement determinations by means of LCK 339 nitrate analysis kits (Dr. Lange Nitrax).

BASIS: Nitrate ions, in presence of sulphuric or phosphoric acid, react with 2,6-dimethylphenol forming 4-nitro-2,6-dimethylphenol which is quantified measuring the absorption at 370 nm.

- Nitrite

Nitrite is measured using UV measurement determinations by means of LCK 341 nitrite analysis kits (Dr. Lange Nitrax).

BASIS: Nitrite ions, in acid solutions, react with primary aromatic amines to form diazone salts which are quantified measuring the absorption at 524 nm.

2.2.2.3 Acetic, butyric and propionic concentrations

Acetic, butyric and propionic acids concentrations are determined either by:

- high resolution liquid chromatography (HPLC) (Hewlett Packard 1050 with an Aminex HPX-87H ionic exchange column and an HP 1047 index refraction detector.
- or gas chromatography (Hewlett Packard 5890).

2.2.2.4 Axenicity control

The fermentors broth and the media are checked for bacterial contamination by optical microscopy (ZEISS AXIOSKOP).

2.2.2.5 Metals concentration determination

- Solid samples

0.3 g of sample are pre-digested during 12 h using 6 mL of HNO_3. Then the digestion takes place in an analytic microwave first heating the sample to 170ºC. The heating is done gradually and the desired temperature is reached after 4 minutes. Then a second gradual temperature increase, that takes 3.5 minutes, is done up to 180ºC. Temperature that is maintained 10 more minutes. The obtained solutions are diluted

with Milli-Q water up to 100mL and then they are filtered. 5 elements (Na, K, Mg, Ca and P) are directly analysed from these solutions using induced coupled plasma emission spectroscopy (ICP-OES). The other elements (B, Mn, Fe, Ni, Cu and Zn) are analysed from 2/10 (2/100 in case of Fe) dilutions using induced coupled plasma mass spectroscopy (ICP-MS). External standards are used in order to quantify the samples.

- Liquid samples

Liquid samples are filtered previously to their analysis. Na, K and Ca are analysed from 1/10 or 1/100 dilutions using ICP-OES and the other elements (Mg, B, P, Mn, Fe, Ni, Cu and Zn) are analysed using ICP-MS after diluting 1/100 the sample. External standards are used in order to quantify the samples.

3 RESULTS AND DISCUSSION

3.1 Artificial media used to connect compartments II, III and IVa that emulates the oucoming media of compartment I

To be able to set the optimal conditions to connect compartments II, III and IVa using the media outcoming from compartment I, this connection is studied using an artificial media containing the same compounds as the media used until now in the connection of these compartments (Creus *et al.*, 1999), but containing the ammonium and the volatile fatty acids concentrations described in table 3.1. This media is presented in table 3.2.

Volatile fatty acids	**g/L**
Acetic acid	0.77
propionic acid	0.27
Butyric acid	0.10
isobutyric acid	0.15
Valeric acid	0.17
Isovaleric acid	0.15
Nitrogen source	N-ppm
Ammonium	414

Table 3.1.- Volatile fatty acids and ammonium concentrations of the outlet media of compartment I.

A5	
Compounds	*g/L*
H_3BO_3	2.860
$MnCl_2 \cdot 4\ H_2O$	1.810
$ZnSO_4 \cdot 7\ H_2O$	0.222
$CuSO_4 \cdot 5\ H_2O$	0.079
MoO_3	0.015

Table 3.2.- Composition of A5 solution

B6	
Compounds	*g/L*
NH_4VO_3	0.023
$KCr(SO_4)_2 \cdot 12\ H_2O$	0.096
$NiSO_4 \cdot 7\ H_2O$	0.048
$(NO_3)_2Co \cdot 6\ H_2O$	0.049
$Na_2WO_4 \cdot 2\ H_2O$	0.018
$Ti(SO_4)_2 + TiOSO_4$	0.048

Table 3.3.- Composition of B6 solution

Trace elements	
Compounds	*g/100mL*
Iron citrate	0.300
$MnSO_4 \cdot H_2O$	0.002
H_3BO_3	0.001
$CuSO_4 \cdot 5\ H_2O$	0.001
$(NH_4)_6MoO_{27} \cdot 4\ H_2O$	0.002
$ZnSO_4$	0.001
EDTA-Na	0.050
$CaCl_2 \cdot 2\ H_2O$	0.020

Table 3.4.- Trace elements solution composition

Biotin	
Compound	*g/L*
Biotin	0.015

Table 3.5.- Biotin solution composition

Product	**1 L**	
Acetic	0,77	g
Propionic	0,27	g
Butyric	0,15	g
Iso-butyric	0,10	g
Valeric	0,17	g
Iso-valeric	0,15	g
EDTA-Na·2 H_2O	0,10	g
$MnCl_2 \cdot 2\ H_2O$	0,01	g
$FeSO_4 \cdot 7\ H_2O$	0,03	g
KH_2PO_4	0,40	g
$NaHCO_3$	0,25	g
$MgSO_4 \cdot 7\ H_2O$	1,20	g
$CaCl_2 \cdot 2\ H_2O$	0,09	g
Trace element	1,00	mL
Biotin	1,00	mL
$(NH_4)_2SO_4$	1,82	g
$CuSO_4.5H_2O$	4,00E-06	g
Na_2HPO_4	0,49	g
$ZnSO_4.7H_2O$	4,30E-06	g
$(NH_4)_6Mo_7O_{27}.4H_2O$	0,18	g
K_2SO_4	0,55	g
A5	1,00	mL
B6	1,00	mL

Table 3.6. - Media composition for the connection tests of compartments II, III and IV. Where the trace element solution, biotin solution, A5 and B6 solutions can be found in tables 3.2, 3.3, 3.4 and 3.5

Carbon source in compartment IV is given by CO_2 bubbling.

Thus, in optimal conditions, when all the volatile fatty acids are consumed in compartment II, theamount of *R. rubrum* produced per litre of incoming media can be calculated following the stoichiometric equations described in TN45.4 (Favier-Teodorescu, L. *et al.*, 1999):

- **Acetic acid** + 0.4115 NH_3 + 0.0299 H_3PO_4 + 0.0066 H_2SO_4 → 1.8550 $CH_{1.6004}O_{0.3621}N_{0.2218}S_{0.0036}P_{0.0161}$ + 0.1450 CO_2 + 1.1843 H_2O

- **Propionic acid** + 0.7201 NH_3 + 0.0523 H_3PO_4 + 0.0116 H_2SO_4 + 0.2462 CO_2 → 3.2462 $CH_{1.6004}O_{0.3621}N_{0.2218}S_{0.0036}P_{0.0161}$ + 1.5726 H_2O

- **Butyric acid** + 1.0287 NH_3 + 0.0748 H_3PO_4 + 0.0165 H_2SO_4 + 0.6374 CO_2 → 4.6374 $CH_{1.6004}O_{0.3621}N_{0.2218}S_{0.0036}P_{0.0161}$ + 1.9609 H_2O

- **Iso-butyric acid** + 1.0287 NH_3 + 0.0748 H_3PO_4 + 0.0165 H_2SO_4 + 0.6374 CO_2 → 4.6374 $CH_{1.6004}O_{0.3621}N_{0.2218}S_{0.0036}P_{0.0161}$ + 1.9609 H_2O

- **Valeric acid** + 1.3373 NH_3 + 0.0972 H_3PO_4 + 0.0215 H_2SO_4 + 1.0286 CO_2 → 6.0286 $CH_{1.6004}O_{0.3621}N_{0.2218}S_{0.0036}P_{0.0161}$ + 2.3491 H_2O

- **Iso-valeric acid** + 1.3373 NH_3 + 0.0972 H_3PO_4 + 0.0215 H_2SO_4 + 1.0286 CO_2 → 6.0286 $CH_{1.6004}O_{0.3621}N_{0.2218}S_{0.0036}P_{0.0161}$ + 2.3491 H_2O

The total amount of biomass calculated to be produced in these conditions is of 1.55 g/l (TN-75.2 Creus *et al.* 2002b).

3.2 Continuous connection of compartments II, III and IVa using artificial media.

Initially, in order to set up the optimal experimental conditions, the connection is done using media that emulates the media outcoming compartment I, see section 3.1. The experimental setup of this connection was presented in section 2.1.

Taking into account the results presented in TN 56.2 (Creus *et al*., 2002a), it was already expected that when increasing the number of the volatile fatty acids given in the inlet media and their carbon number, *R.rubrum* growth rate decreases if the same energy is supplied. Thus, the initial experimental conditions tested, presented in table 3.7, assume the need to supply the maximum energy to the culture and testing a dilution rate lower than the maximum dilution rate tested in TN 56.2, which is D=0.0148 h^{-1}. This takes into account that in this experiment the number of volatile fatty acids is bigger and the amount of gC/L_{medium} is higher.

	Compartment II
Light (W/m^2)	720
D (h^{-1})	0.0092
Q_L (mL/day)	88
τ (days)	4.5

Table 3.7.- Initial conditions of compartment II.

The evolution of compartment II using these conditions is presented in figure 3.1. As can be seen in that figure, the culture does not handle these conditions and biomass decreases. This biomass decrease can be either due to some inhibitory effects or to too difficult experimental conditions. In figure 3.6 the theoretical biomass wash out curve is represented. From this representation some *R. rubrum* growth is observed as the experimental results are always above the theoretical wash out curve. Thus, if the washing effect is due to too hard experimental conditions the theoretical maximum *R. rubrum* growth in these experimental conditions is found as follows.

As the reactor is not operating at the steady state the biomass mass balance is described as follows:

$$\frac{dX}{dt} = D(X_0 - X) - \mu X \qquad (1)$$

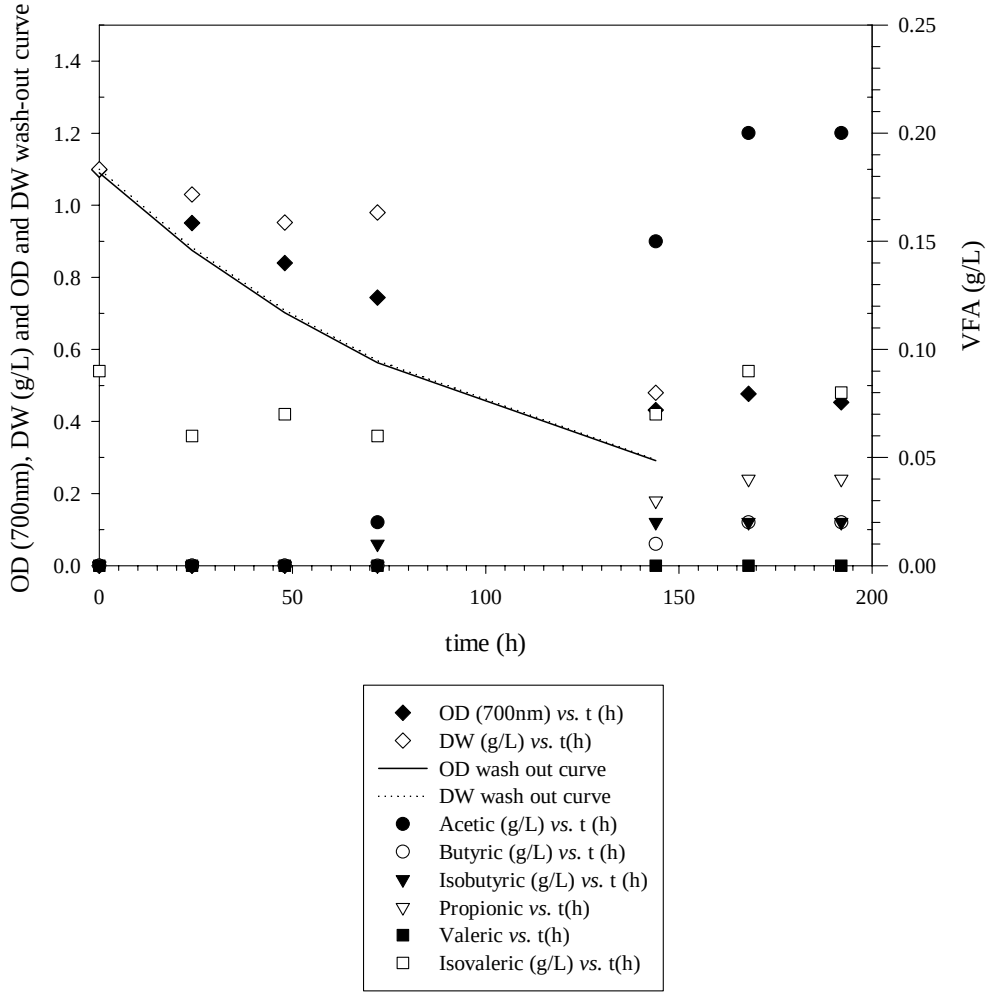

Figure 3.1.- Evolution of compartment II using the experimental conditions described in table 3.7.

Taking into account that $X_0 = 0$ as no biomass is present in the inlet, equation 1 becomes equation 2:

$$\frac{dX}{dt} = -(D+\mu)X \qquad (2)$$

Equation 2 directly leads to equation (3)

$$\frac{dX}{X} = -(D+\mu)dt \qquad (3)$$

Integrating equation 3, equation 4 is obtained:

$$\ln\frac{X}{X_0} = -(D+\mu)(t-t_0) \qquad (4)$$

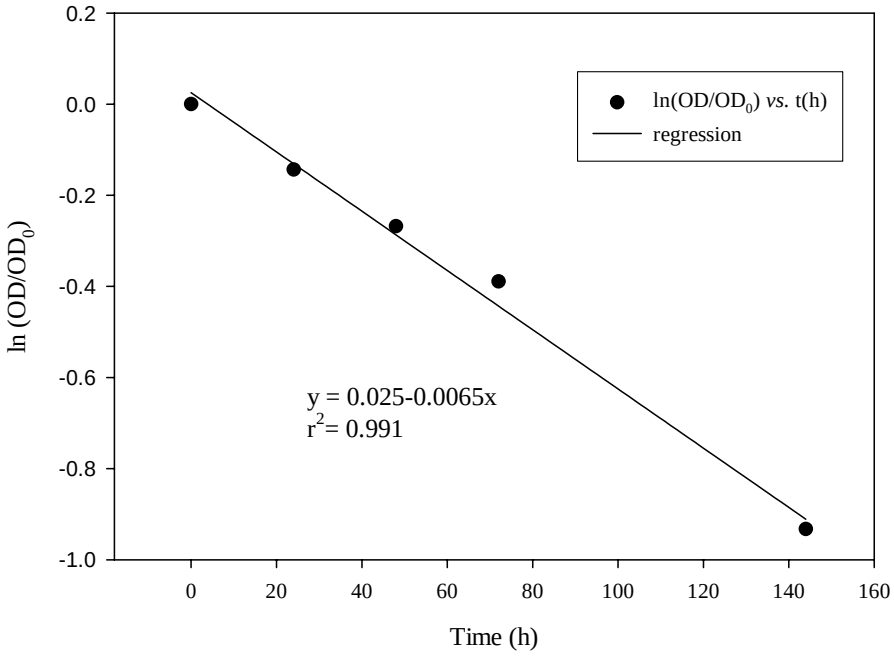

Figure 3.2.- Representation of ln (OD/OD0) vs. t in order to find the experimental μ for the experiment in figure 3.6

Thus, representing $\ln(X/X_0)$ *vs* $t\text{-}t_0$, $D+\mu$ is calculated from the slope. And taking into account that the dilution rate of the experiment is known the experimental μ is found, as seen in figure 3.2. From that figure the experimental μ is found: $\mu = 0.0027$. Thus, taking into account that at steady state: $\mu = D$, a new experiment with the calculated dilution rate is performed. These new conditions are presented in table 3.8.

	Compartment II	
	I	*II*
Light (W/m^2)	78	724
D (h^{-1})	BATCH	0.0027
Q_L (mL/day)		26.7
τ (days)		15

Table 3.8.- Conditions of compartment II

The evolution of compartment II under these new conditions is presented in figure 3.3.

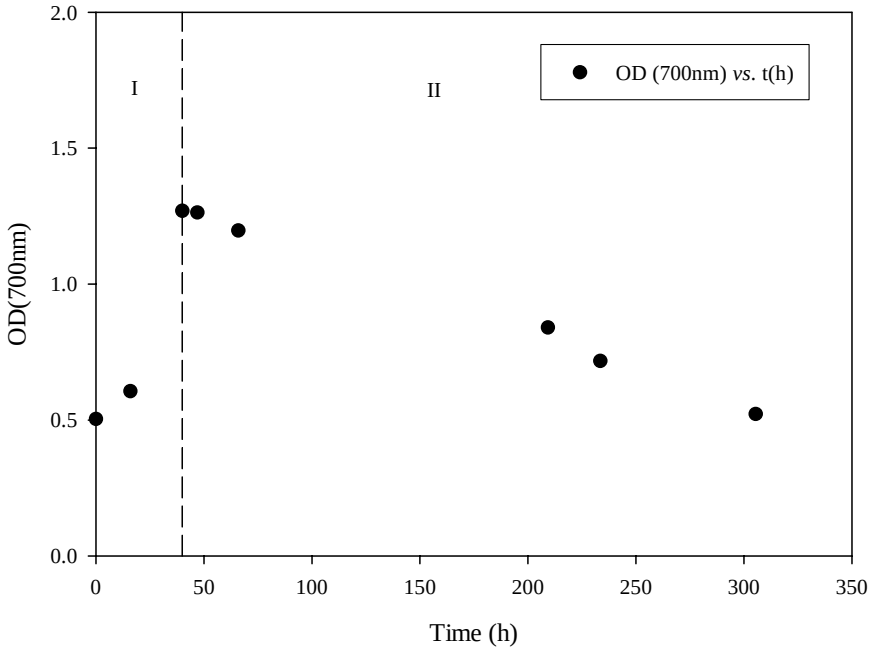

Figure 3.3.- Evolution of compartment II using the experimental conditions presented in table 3.8.

As it is seen in figure 3.3, *R. rubrum* does not handle these conditions, thus, a growth inhibition is observed. Taking into account that it grows well during the batch mode and that the only different factor between the batch and the continuous mode is the amount of incident light, it seems that light is the factor inhibiting *R. rubrum* growth. Until now, no light inhibition effect had been described in *R. rubrum* cultures except in the test tube cultures performed by Albiol, (Albiol, 1994) where due to the concurrent effect of too high temperatures it could not be completely described. However, light inhibition is described in almost all the photosynthetic cultures. What is more, the bioreactor used in these experiments is able to supply a higher F_R than anyone else tested before and its radius is smaller. Consequently, $4\pi j$ values are surely the highest ever tested. Thus, a new experiment using the conditions described in table 3.9 is done.

	Compartment II						
	I	*II*	*III*	*IV*	*V*	*VI*	*VII*
Light (W/m^2)	724	78	78	78	137	137	137
D (h^{-1})	BATCH	BATCH	0.018	0.031	0.093	0.145	0.208
Q_L (mL/day)			168.75	300	900	1400	2000
τ (days)			2.37	1.33	0.44	0.29	0.2

Table 3.9.- Conditions of compartment II

The evolution of compartment II under these conditions is found in figure 3.4, where the biomass is followed, and 3.5, where the outlet of ammonium and VFA are followed.

As figures 3.4 and 3.5 show, and as expected from previous data, an excess of light inhibits *R. rubrum* growth. During conditions I, supplying the maximum amount of light available to the fermentor, *R. rubrum* does not grow, and it starts growing, when the light is highly decreased, conditions II. Then, the continuous mode is perfectly maintained even using really high dilution rates. Dilution rates similar to the maximum dilution rate obtained using only acetic acid as carbon source, TN 47.5 (Creus *et al.*, 2001), and much higher than the maximum dilution rate obtained using acetic, propionic and butyric acids as carbon sources in TN 52.6 (Creus *et al.*, 2002). These facts, stress the point that light is one of the most important factors in *R. rubrum* growth. A shortness of light, energy, strongly decreases *R. rubrum* maximum growth rate and an excess of light highly inhibits its growth.

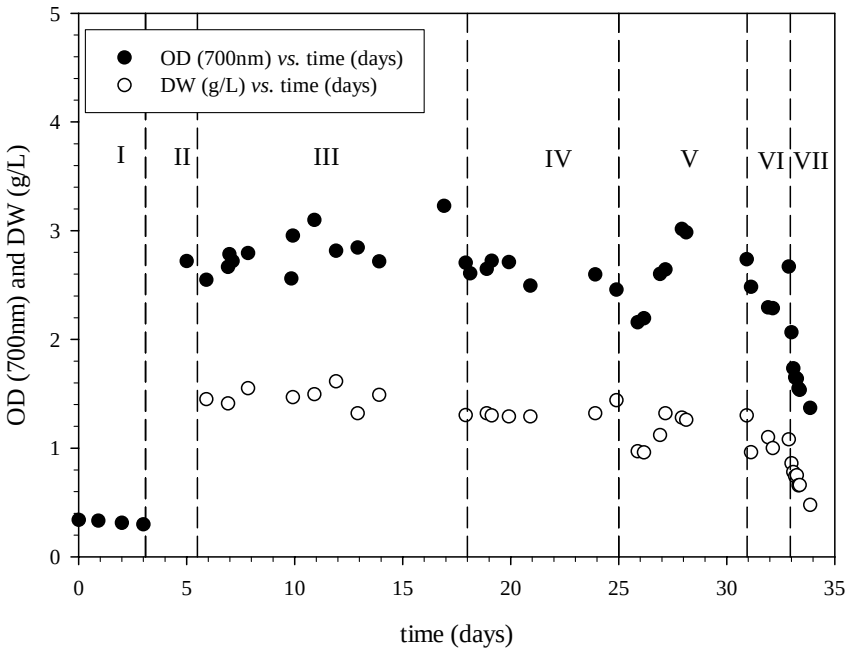

Figure 3.4.- Evolution of the biomass of compartment II during the conditions presented in table 3.14.

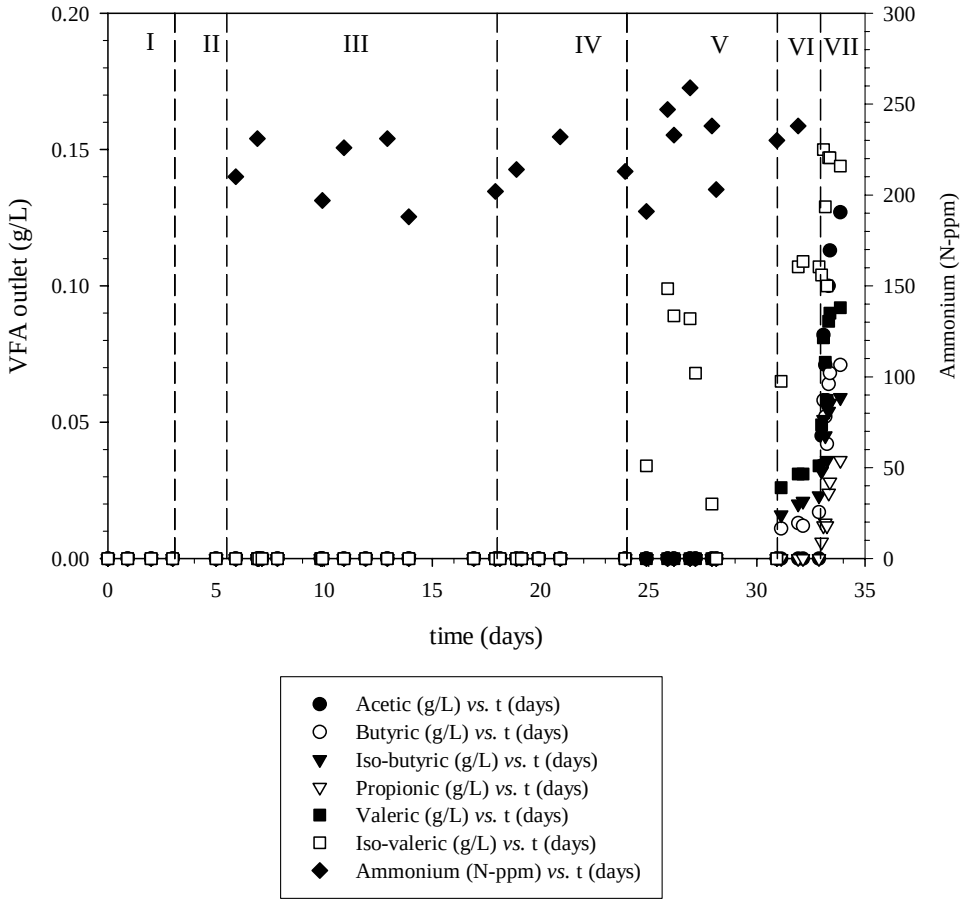

Figure 3.5.- Evolution of the outleting ammonium and VFA concentrations of compartment II during the conditions presented in table 3.14.

As it is seen in figures 3.4 and 3.5, using conditions III and IV, compartment II operates at its optimal stage, thus, no VFA are found in its outlet. The same can be said when conditions V are used as the iso-valeric acid peak found, see figure 3.5, is only a transitory effect due to the dilution rate increase.

Using conditions VI a steady state is reached where butyric, iso-butyric, valeric and iso-valeric acids are present in the outlet of this compartment. As expected, the volatile fatty acids completely consumed are, acetic and propionic acids, the VFA with a lower C-chain. In previous experiments, see TN 47.5 (Creus *et al*., 2001), it was observed that when acetic acid is present in the outlet of compartment II, *R. rubrum* accumulates PHB, looses its mobility and presents cell division problems. These problems are not observed when butyric, iso-butyric, valeric and iso-valeric acids are in excess, and this fact is perhaps due to a lower *R. rubrum* PHB production with these VFA.

Conditions VII are set in an attemp to find the maximum *R. rubrum* growth rate. The light supplied and other conditions are described in table 3.9, From equation 4, section 3, and representing $\ln(X/X_0)$ *vs* $t\text{-}t_0$, $D+\mu$ is found. And taking into account that the dilution rate of the experiment is known the experimental μ is achieved, as seen in figure 3.6.

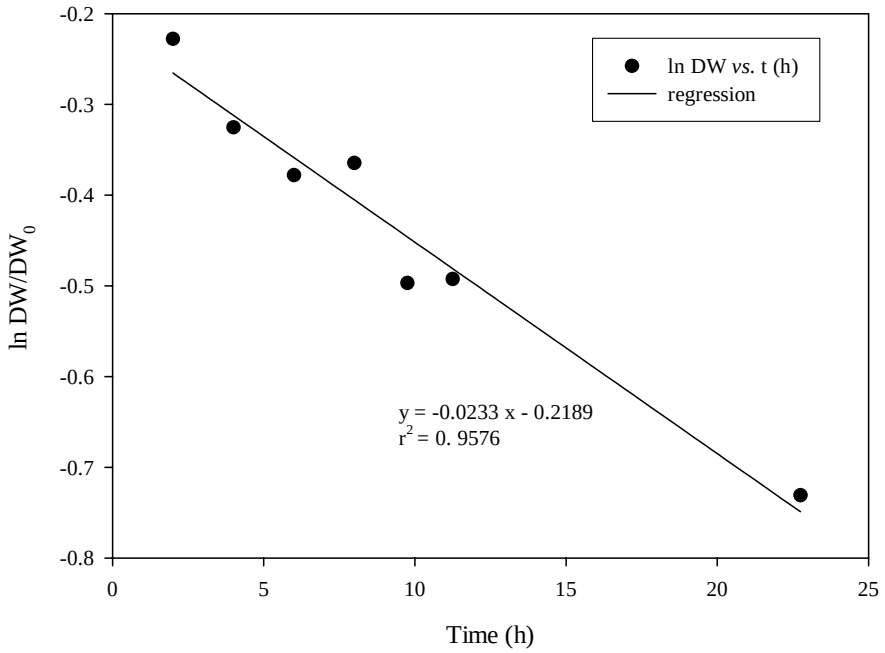

Figure 3.6.- Representation of ln (DW/DW_0) vs. time in order to find the μ_{max} experimental.

Thus, the maximum *R. rubrum* growth rate, at these conditions, is $\mu_{max} = 0.17h^{-1}$. This value is rather high and similar to the maximum *R.rubrum* growth rate achieved in previous experiments, using only acetic acid as carbon source ($0.15h^{-1}$ in continuous cultures and $0.17h^{-1}$ in test tubes) (Albiol, 1994).

During conditions III, IV and V the carbon and nitrogen balances can be easily done., During these conditions, as seen in figure 3.4, about 1.4 g DW/L are found, thus a 90 % of the expected biomass is formed taking into account that with this inlet media (section 3.1) 1.55 g DW/L should be produced. A production of 1.4 g DW/L of *R. rubrum* requires about 194 N-ppm if the *R. rubrum* elemental composition presented in section 3.1 is considered. The nitrogen consumed in compartment II during this experiment is of about 194 N-ppm as the inlet media contains 414 N-ppm and in the outlet about 220 N-ppm are found, figure 3.5. Thus the nitrogen balance can also be considered closed.

The outlet of compartment II, during conditions III, IV and V, when no iso-valeric acid is found in the outlet, is introduced first in compartment III and then in compartment IVa in order to evaluate the connection of these three compartments.

The experimental conditions of compartment III and IVa during the connection is found in table 3.10 and the evolutions of these compartments during this experiment are presented in figures 3.7 and 3.8.

	Compartment III	*Compartment IVa*
F_R *(W/m^2)*	-	94
Q_L *(mL/day)*	400	400
D *(h^{-1})*	0,035	0,042
ι *(days)*	0,84	1

Table 3.10.- Experimental conditions of compartments III and IVa used during the connection of compartments II, III and IVa.

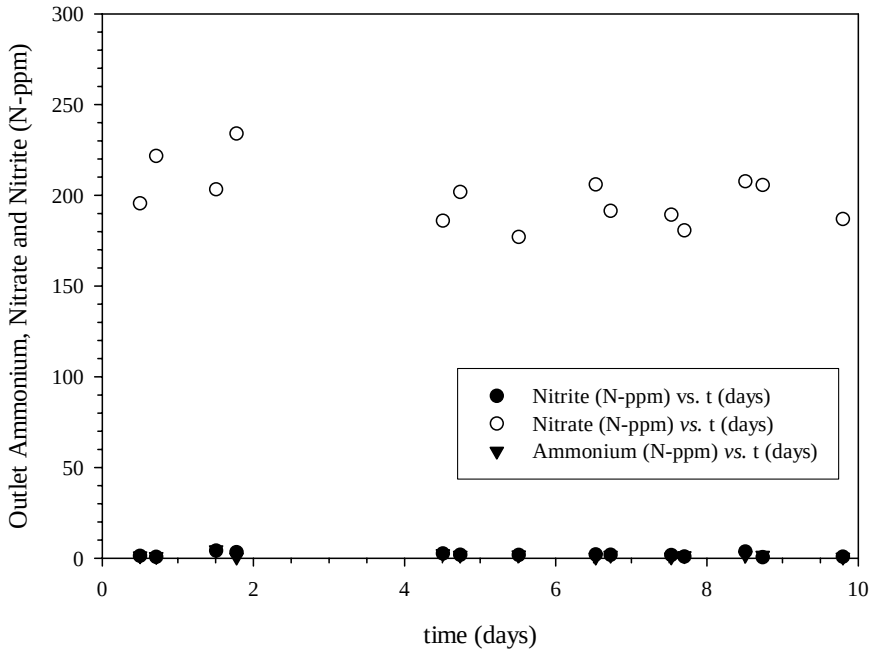

Figure 3.7.- Evolution of compartment III using conditions described in table 3.10.

Compartment III behaves at its optimal conditions as can be seen in figure 3.12.

All the incoming Nitrogen from ammonium, about 200 N-ppm that are found in the outlet of compartment II, see figure 3.7, and are converted to nitrate and neither ammonium nor nitrite are found in the outlet.

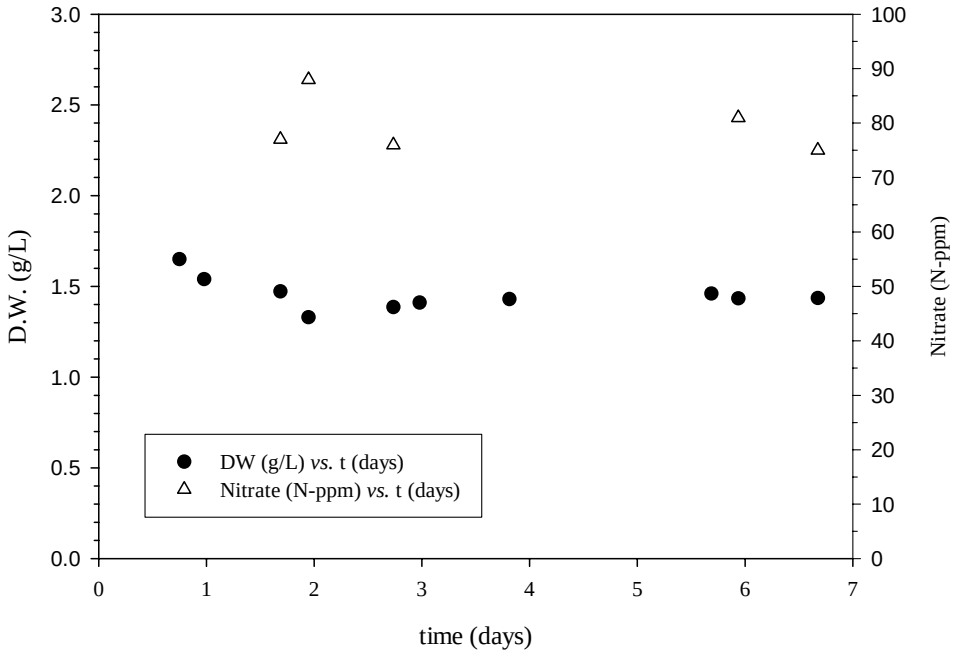

Figure 3.8.- Evolution of compartment IVa using conditions described in table 3.10

As it is seen in figure 3.8 compartment IVa has a complete stable situation. A steady state at about 1.43 g DW/L is reached and non-toxic effects are observed.

The carbon balance of this compartment cannot be done, as the major carbon source is the CO_2 bubbled in the fermentor, which is introduced in excess and is not measured in the outlet.

Considering the *S.platensis* elemental composition:$CH_{1.650}O_{0.531}N_{0.170}S_{0.007}P_{0.006}$, (Cornet, 1992), in order to produce 1.43 g DW/L 136 N-ppm are required. In figure 3.13 a nitrogen consumption of 120 N-ppm is found taking into account the nitrogen income of compartment IVa, figure 3.12. Thus, the nitrogen balance can also be considered closed.

In this section the experimental conditions, with which the connection of compartments II, III and IVa using the new set-up, and using a media emulating the outcoming media of compartment I can be performed, have been set. The connection of these compartments has been done without presenting any major difficulties and without showing any kind of toxicity in none of the reactors.

A strong light effect has been observed in compartment II. An excess of light inhibits *R. rubrum* growth and a low light availability strongly diminishes its maximum growth rate.

4 CONCLUSIONS

As a summary of the previously described tests, the following can be concluded:

- The feasibility of the connection of compartments II, III and IVa using a media containing the same concentration of volatile fatty acids and ammonium of the medium outcoming from compartment I has been demonstrated.

- A strong light effect in *R. rubrum* growth has been observed. An excess of light inhibits its growth and a low light availability strongly diminishes its maximum growth rate. The effect of light intensity on the growth rate of *R.rubrum* will be more deeply evaluated using the light distribution model under development.

5 REFERENCES

Albiol, J. (1994) Study of the MELISSA photoheterotrophic compartment. Kinetics and effects of C limitation. ESA/YCL/2148.JAS.ESA-EWP-1808.

Cornet J.F., Dussap C.G. and Duberet G., 1992a. A structured model for simulation of cultures of the cyanobacterium *Spirulina platensis* in photobioreactors: I. Coupling between light transfer and growth kinectics. Biotechnol,40, 817-825.

Cornet J.F., Dussap C.G., Cluzel P- and Duberet G., 1992b. A structured model for simulation of cultures of the cyanobacterium *Spirulina platensis* in photobioreactors: II. Identification of kinectic parameters under light and mineral limitations. Biotechnol Bioeng, 40, 826-834.

Creus, N., Albiol, J. and Gòdia, F. (1999) Preliminary connection between 3 compartments. Technical Note 43.8. ESTEC/CONTRACT11549/95/NL/FG.

Creus, N., Albiol, J. and Gòdia, F. (2001) Tests with the 3 linked bench compartments. Technical Note 47.5. ESTEC/CONTRACT13292/98/NL/MV.

Creus, N., Albiol, J. and Gòdia, F. (2002a) Tests with the 3 linked bench compartments using 3 different carbon sources Technical Note 52.6. ESTEC/CONTRACT13292/98/NL/MV.

Creus, N., Albiol, J. and Gòdia, F. (2002b) Bench scale loop tests using compartment I outlet medium. Technical Note 75.2. ESTEC/CONTRACT13292/98/NL/MV.

Favier-Teodorescu, L., Pons, A., and Poughon, L. (1999) Stoichiometric analysis of *R. rubrum* growth on different carbon substrates. Technical Note 45.4. ESTEC/CONTRACT 13323/98/NL/MV.

Godia, F., Albiol, J., Creus, N. and Perez, J. (2001) Preliminary Review of the Pilot Plant Integration Loop. Technical Note 47.3. ESA contract ESTEC/CONTRACT13292/98/NL/MV.

Hermans, V. and Demey, D. (1998). Detailed characterization of the thermophilic biodegradation process. Technical note 41.2. ESA contract 12922/98/NL/MV.

Hermans, V. and Demey, D. (2001). Biodegradation of non edible parts of plants and bacterial biomass. Technical note 56.2. ESA contract 12922/98/NL/MV.

Mohanty, P., Srivastava, M. and Kishna, K.B. (1997) In: *Spirulina platensis* (*Arthrospira*): Physiology, Cell-biology and Biotechnology. Vhonsak A. (ed) London, 233p.

Montràs, A., Pérez, J. ,Gòdia, F. (2001) On-line Instrumentation for N balance. Techinal Note 52.21. ESTEC CONTRACT 11549/95/NL/FG.

Pérez, J. (1997) Caracterización y puesta a punto de reactores de lecho fijo para su aplicación en procesos de nitrificación. Magister tesis. Universitat Autònoma de Barcelona.

Poughon, L (1997) Including of a Higher Plants Chamber in the MELISSA loop description of a HPC for MELISSA loop steady state simulations. Technical Note 32.3. ESA/ESTEC P.O.; 161081

6 APPENDIX I. -LIGHT CALIBRATION OF COMPARTMENT II

The light availability determination is of key importance for the operation of photobioreactors. Once light intensity at the bioreactor's surface is known, the light availability at any point of the bioreactor can be determined.

The light intensity at the bioreactor's surface is obtained by measuring the light intensity at the axis of the bioreactor, using a spherical light sensor that integrates the light reaching its radial illuminated surface. Conversion of the light intensity measured by the spherical sensor to the light intensity at the surface of the bioreactor is done using the following equation:

$$Fr = \frac{Eb \cdot rb}{\pi \cdot Rb}$$

Where: Fr is the light flux at the bioreactor's surface, Eb is the light intensity measured by the sensor, rb is the sensor's radius (30mm) and Rb is the bioreactor's radius (31mm).

The available light measured by the sensor is given in mols/m2s. For the application of the previously developed light transfer mathematical models, it is necessary to convert the units of the sensor to W/m^2. The conversion coefficient used is 0.425, which has been previously calculated by J.F.Cornet by integration of the used lamps spectra in the range 350–950nm used by *Rhodospirillum rubrum*.

The Eb values are measured in the empty bioreactor with water circulating through the external jacket.

Light intensity measurements are done at different vertical positions and at different voltages supplied to the lamps. The results of these measurements are plotted in figure I.1.

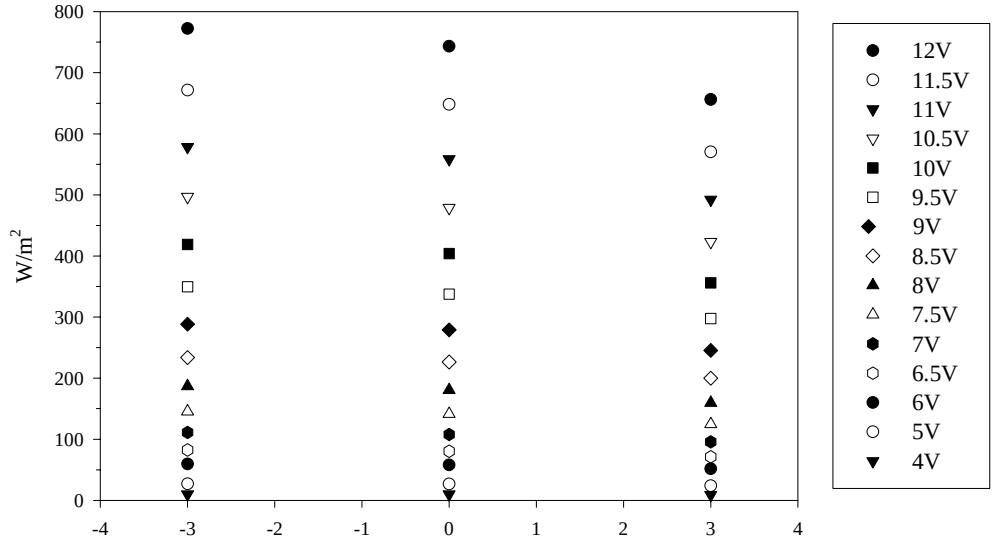

Figure I.1.- Light intensity at different vertical positions supplying different voltages (assuming 0 cm the centre of the reactor).

Averaging the measurements obtained at different vertical positions, the mean light intensity value for each voltage supplied to the lamps is obtained. The light intensity values measured by the sensor in μmols/m^2s, are converted to Fr values in W/m^2 using the above mentioned formula and conversion factor. Figure I.2 shows the relationship between the voltage supplied to the lamps and the Fr of the bioreactor.

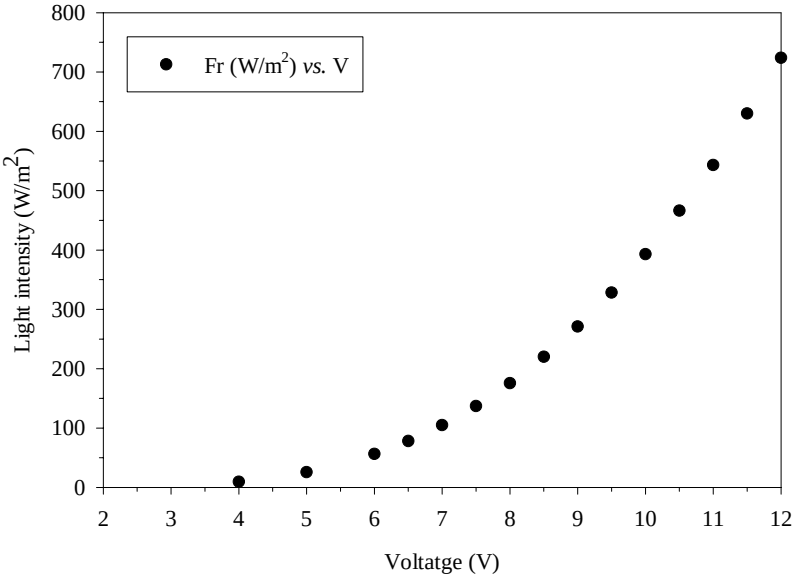

Figure I.2 .- Average light intensity supplying different voltages

7 APPENDIX II. -LIGHT CALIBRATION OF COMPARTMENT IVA

The determination of the light intensity at the bioreactor's surface is done as previously described in Appendix I . In this case, the Rb (radius of the bioreactor) is also 31mm. The conversion factor is 0.291, which has been calculated by J.F. Cornet by integration of the used lamps spectra in the range 350-750 nm used by *Spirulina platensis* cells. The results obtained by measuring light intensity at different vertical positions and supplying different voltages to the lamps are plotted in figure II.1.

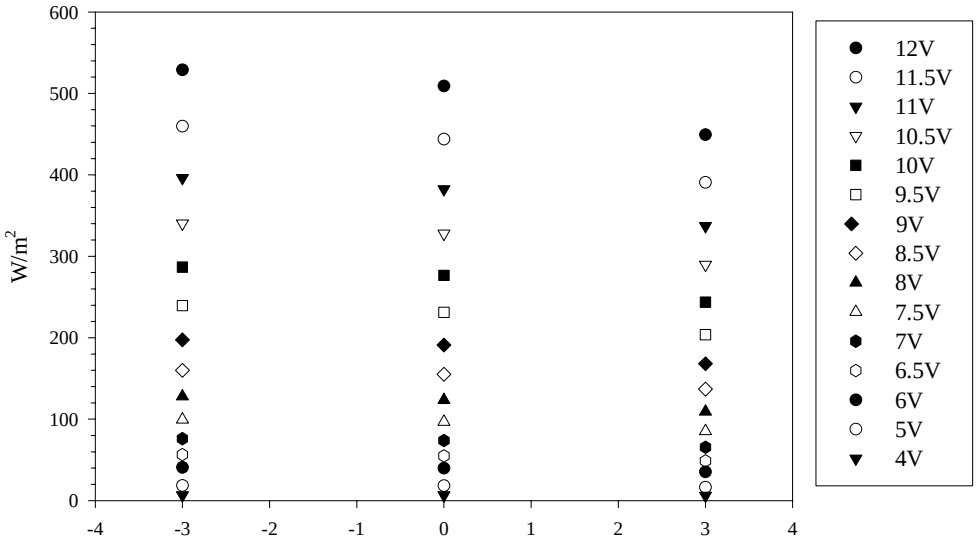

Figure II.1.- Light intensity at different vertical positions supplying different voltages (assuming 0cm the centre of the reactor)

The average relationship between the voltage supplied to the lamps and the Fr of the bioreactor obtained is presented in figure II.2.

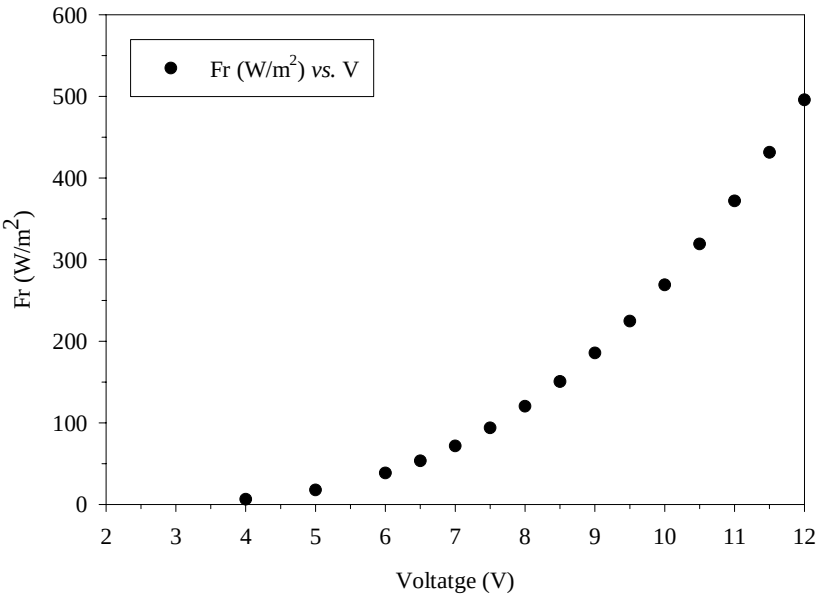

Figure II.2.- Average light intensity